BIOCHEMISTRY
including biophysical chemistry & molecular biology

Article

pubs.acs.org/biochemistry

Structural Insights into the Conformation and Oligomerization of E2∼Ubiquitin Conjugates

Richard C. Page,*[,†] Jonathan N. Pruneda,[‡] Joseph Amick,[†] Rachel E. Klevit,[‡] and Saurav Misra*[,†]

[†]Department of Molecular Cardiology, Lerner Research Institute, Cleveland Clinic, 9500 Euclid Avenue, Cleveland, Ohio 44195, United States.

[‡]Department of Biochemistry, University of Washington, Seattle, Washington 98195, United States.

Supporting Information

ABSTRACT: Post-translational modification of proteins by ubiquitin (Ub) regulates a host of cellular processes, including protein quality control, DNA repair, endocytosis, and cellular signaling. In the ubiquitination cascade, a thioester-linked conjugate between the C-terminus of Ub and the active site cysteine of a ubiquitin-conjugating enzyme (E2) is formed. The E2∼Ub conjugate interacts with a ubiquitin ligase (E3) to transfer Ub to a lysine residue on a target protein. The flexibly linked E2∼Ub conjugates have been shown to form a range of structures in solution. In addition, select E2∼Ub conjugates oligomerize through a noncovalent "backside" interaction between Ub and E2 components of different conjugates. Additional studies are needed to bridge the gap between the dynamic monomeric conjugates, E2∼Ub oligomers, and the mechanisms of ubiquitination. We present a new 2.35 Å crystal structure of an oligomeric UbcH5c∼Ub conjugate. The conjugate forms a staggered linear oligomer that differs substantially from the "infinite spiral" helical arrangement of the only previously reported structure of an oligomeric conjugate. Our structure also differs in intraconjugate conformation from other structurally characterized conjugates. Despite these differences, we find that the backside interaction mode is conserved in different conjugate oligomers and is independent of intraconjugate relative E2−Ub orientations. We delineate a common intraconjugate E2-binding surface on Ub. In addition, we demonstrate that an E3 CHIP (carboxyl terminus of Hsp70 interacting protein) interacts directly with UbcH5c∼Ub oligomers, not only with conjugate monomers. These results provide insights into the conformational diversity of E2∼Ub conjugates and conjugate oligomers, and into their compatibility and interactions with E3s, which have important consequences for the ubiquitination process.

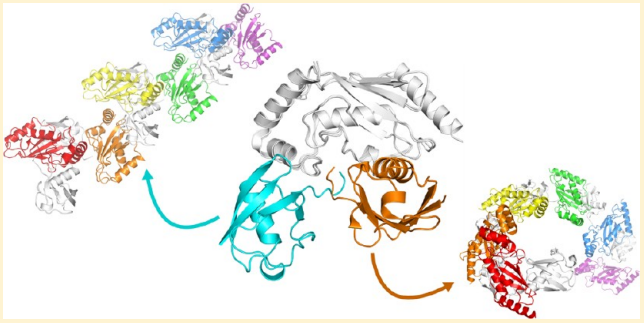

Ubiquitination is a widely utilized post-translational modification that regulates numerous cellular processes.[1−3] In the initial step of a ubiquitination cascade, the C-terminus of ubiquitin (Ub) is activated in an ATP-dependent manner by a ubiquitin-activating enzyme (E1). The C-terminus of Ub is thereupon linked to the E1 active site cysteine through a thioester bond and subsequently transferred to the active site cysteine of a ubiquitin-conjugating (E2) enzyme.[1] The resulting thioester-linked E2∼Ub conjugate interacts with a ubiquitin ligase (E3), which also binds to a target protein. RING- or U-box-type E3s promote the direct transfer of Ub from the E2∼Ub conjugate to a target protein lysine, resulting in the formation of an isopeptide bond between the lysine ε-amino group and the C-terminus of Ub.[4,5] In contrast, HECT- or RING-in-between-RING (RBR)-type E3s promote the transfer of Ub to an active site cysteine of the E3 followed by subsequent formation of an isopeptide bond between Ub and a substrate lysine.[6,7] In some cases, the substrate N-terminal amine, rather than an internal lysine, is ubiquitinated.[8] In addition to target protein lysines, the ε-amino group of any of the seven lysines within Ub or the amino terminus of Ub can be ubiquitinated, leading to the formation of linear or branched polyubiquitin chains.[9] The well-studied Lys48-linked polyubiquitin chain is utilized for protein degradation by the 26S proteasome.[1] Other polyubiquitin chains participate in a variety of cellular pathways; for example, Lys63-linked chains regulate DNA repair and transcription.[1,3]

In general, the topology of an elongating polyubiquitin chain is determined by the identity of both the E2 and the E3.[5,10−12] The human genome encodes approximately 35 E2s and hundreds of E3s. E3s are known to simultaneously bind the E2∼Ub conjugate and target protein, but the mechanism of Ub transfer remains elusive. A number of studies have examined conformational changes within E3s that may bring target lysine residues near the active site of the E2∼Ub conjugate.[13−16] In addition, E3s are known to increase the rate of release of Ub from the E2∼Ub conjugate, even in the absence of a target protein.[7,17] E3 enzymes may directly influence the conforma-

Received: January 13, 2012
Revised: May 1, 2012
Published: May 2, 2012

tions of key catalytic residues in the active site of the E2∼Ub conjugate to enhance the Ub release rate.

While E3s adopt multiple, divergent architectures, E2 enzymes share a conserved α/β topology.[18] While structural characterization of conjugates is substantially more challenging than characterization of free E2 enzymes, there are now five structures of E2∼Ub conjugates in the Protein Data Bank (PDB). Crystal structures include those of the Ubc13∼Ub conjugate in complex with Mms2 (PDB entry 2gmi),[19] the UbcH5b∼Ub conjugate in complex with NEDD4L-HECT (PDB entry 3jw0),[20] and an isolated UbcH5b∼Ub conjugate (PDB entry 3a33).[21] NMR structural models of E2∼Ub conjugates, based on Monte Carlo docking using NMR chemical shift perturbation or cross saturation data, include those of the thioester-linked Ubc1∼Ub conjugate (PDB entry 1fxt)[22] and a disulfide-linked UbcH8−S−S−Ub conjugate (PDB entry 2kjh).[23] The backbone structures of the E2 and Ub moieties in the conjugates do not deviate significantly from isolated E2 or Ub structures. However, the orientations of Ub relative to the E2 vary distinctly between these structures. The conformational landscape of E2∼Ub conjugates in solution has only recently been examined.[24] Analysis of UbcH5c∼Ub and Ubc13∼Ub conjugates by NMR and small-angle X-ray scattering (SAXS) shows that UbcH5c∼Ub and Ubc13∼Ub conjugates exhibit a range of conformations in solution.[24]

Intriguingly, conjugates of a subclass of E2 enzymes form oligomers in solution.[25−30] This oligomerization is mediated by the *trans* interaction of the Ub of one conjugate with a so-called "backside" interaction surface on the E2 enzyme of another conjugate. Mutagenic disruption of this interaction prevents oligomerization but also greatly inhibits the ability of these E2 enzymes to generate polyubiquitin chains, suggesting that oligomerization facilitates ubiquitin chain extension.[25] Oligomerization may be another mechanism that allows distally located substrate lysines or growing ubiquitin chains to access E2∼Ub conjugates. In addition, there is evidence that the backside interaction may modulate the E2 active site and promote catalysis and ubiquitin transfer directly.[21,29] Oligomerization and the backside interaction were initially identified and characterized by solution NMR techniques. Subsequently, a crystal structure of a UbcH5b∼Ub conjugate (PDB entry 3a33) exhibited this interaction in the context of the crystal lattice.[21] A resulting "infinite spiral" oligomeric arrangement of conjugates in this lattice was proposed to accurately represent the state of the conjugate oligomer in solution. It was unclear whether conjugate oligomers exclusively adopt this spiral arrangement.

Additional examinations of the relation among E2∼Ub conformations, E2 active site conformation, and conjugate oligomerization would provide clues about the activation of E2∼Ub conjugates by E3s and about how substrates access these conjugates. In this report, we describe a new crystal structure of the UbcH5c∼Ub conjugate in space group $P12_11$ at 2.35 Å resolution. The structure shows both a new intraconjugate conformation and a novel staggered linear oligomeric arrangement mediated through the canonical backside interaction. Our structure of the UbcH5c∼Ub conjugate demonstrates that UbcH5∼Ub oligomerization does not require a specific relative intraconjugate Ub orientation. Our structure also suggests that extensive conformational variability is accommodated, and likely present, in conjugate oligomers. Docking of oligomeric conjugates onto E3 structures shows that neither oligomeric arrangement conflicts sterically with even relatively large ligases. By comparing the structure of the UbcH5c∼Ub conjugate to structures of other E2∼Ub conjugates, we identify a common Ub surface used in intraconjugate E2−Ub interactions. Finally, we show that the E3 CHIP (carboxyl terminus of Hsp70 interacting protein) interacts directly with UbcH5c∼Ub oligomers in solution, showing that E3s may indeed recruit such oligomers to facilitate polyubiquitination.

EXPERIMENTAL PROCEDURES

Protein Expression, Purification, and Formation of the UbcH5c∼Ub Conjugate. Protein expression in *Escherichia coli* (BL21 star DE3) was induced by 200 μM IPTG followed by shaking for 18 h at 16 °C. Human UbcH5c (HsUbcH5c) was expressed from the pET28N vector (available from Addgene.org) and purified as previously described.[31] Human UbcH5b (HsUbcH5b) and human full-length CHIP [His_6-HsCHIP(1−303)] were expressed from pGST-parallel-2 and pHis-parallel-2 vectors, respectively, and purified as previously described.[32] Reactions to produce the UbcH5c∼Ub or UbcH5b∼Ub conjugate utilized active site Cys-to-Ser (C85S) mutants of the respective E2 enzymes to generate oxyester-linked E2∼Ub conjugates. Ser-to-Arg (S22R) mutations were added to the UbcH5 enzymes to produce oligomerization deficient E2∼Ub conjugates.[25] Conjugation reactions were perfomed by mixing 10 μM human E1, 600 μM mammalian Ub, 300 μM E2 enzyme [HsUbcH5c(C85S), HsUbcH5b-(C85S), or HsUbcH5b(C85S/S22R)], 5 mM $MgCl_2$, and 2.5 mM ATP followed by incubation at 30 °C for 6 h. The UbcH5∼Ub conjugate was purified from conjugation reactions by gel filtration on Superdex 75 resin (GE Healthcare) equilibrated with 25 mM HEPES (pH 7) and 50 mM NaCl. The purity of UbcH5∼Ub gel filtration fractions was assessed by sodium dodecyl sulfate−polyacrylamide gel electrophoresis (SDS−PAGE). The UbcH5∼Ub conjugate was concentrated to 0.9 mM prior to its use in crystallization trials.

Crystallization and X-ray Data Collection. Crystals of the human UbcH5c(C85S)∼Ub oxyester conjugate were grown by sitting drop vapor diffusion at 293 K in 0.4 μL drops. Sitting drops, consisting of a 1:1 ratio of the UbcH5c∼Ub conjugate (0.9 mM) and a reservoir solution, were prepared using a Crystal Gryphon liquid handling robot (Art Robbins Instruments). Initial screening was conducted using the sparse-matrix crystallization screens JCSG Core I−IV (Qiagen). Optimization of initial screening hits identified an optimal reservoir solution that consisted of 200 mM tripotassium citrate and 20% PEG 3350. Resulting single crystals were cryoprotected in LV CryoOil (MiTeGen). X-ray diffraction data were collected with a Cu Kα source (1.5418 Å wavelength) using a Rigaku MicroMax-007HF generator and a Rigaku Saturn 944+ CCD detector. Data reduction was conducted using *d*TREK*.[33]

Structure Solution and Refinement. Phases for the 2.35 Å data set were calculated by molecular replacement utilizing the *PHASER*[34] component of *PHENIX*[35] using the following search models: PDB entry 3tgd for UbcH5c and PDB entry 1ubq for Ub. A single molecular replacement solution was found in space group $P12_11$. The molecular replacement solution was subjected to automated rebuilding in *PHENIX* with *RESOLVE*,[36] followed by rounds of iterative refinement (*PHENIX*) and model building in *COOT*.[37] The refinement protocol used isotropic atomic displacement parameters for all atoms and TLS motion analysis for protein chains.[38] All

dx.doi.org/10.1021/bi300058m | *Biochemistry* 2012, 51, 4175−4187

molecular structure figures were prepared with *PyMOL*.[39] The atomic coordinates and structure factors have been deposited in the PDB (entry 3ugb). Stereochemical and geometric analyses of the structure of the UbcH5c∼Ub conjugate were performed using *MolProbity*.[40,41]

UbcH5∼Ub Conjugate Pull-Down Assays. Full-length His_6-HsCHIP(1−303) was bound to His Mag Sepharose Ni resin (GE Healthcare) by incubation of 40 μL of a resin suspension with 20 μL of 20 μM His_6-HsCHIP(1−303) for 2 h at 4 °C in 25 mM HEPES (pH 7), 150 mM NaCl, and 5 mM imidazole. Unbound CHIP was removed by washing the His Mag Sepharose Ni resin with four separate washes of bead wash buffer [500 μL of 25 mM HEPES (pH 7), 150 mM NaCl, and 5 mM imidazole]. Increasing volumes of 20 μM HsUbcH5b(C85S)∼Ub or 20 μM HsUbcH5b(C85S/S22R)∼Ub conjugate were added to tubes containing full-length CHIP bound to His Mag Sepharose Ni resin and incubated for 3 h at 4 °C in bead wash buffer. The unbound UbcH5b∼Ub conjugate was removed by washing the samples with 500 μL of wash buffer. Protein was eluted from His Mag Sepharose Ni resin by addition of 30 μL of 25 mM HEPES (pH 7), 150 mM NaCl, and 500 mM imidazole. SDS−PAGE samples were separated on a 12.5% polyacrylamide gel. UbcH5b∼Ub conjugate input lanes were loaded with 10 μL of a sample comprised of 20 μL of 2× SDS−PAGE buffer (Fisher) and 20 μL of 20 μM UbcH5b∼Ub conjugate. CHIP input lanes were loaded with 10 μL of a sample comprised of 30 μL of 2× SDS−PAGE buffer and 30 μL of CHIP eluted from His Mag Sepharose Ni resin. All other lanes were loaded with 10 μL of 30 μL of 2× SDS−PAGE buffer and 30 μL of a CHIP/UbcH5∼Ub mixture eluted from His Mag Sepharose Ni resin. Following electrophoresis, gels were stained with IRDye Blue Protein Stain (LI-COR) and imaged using an Odyssey infrared imaging system (LI-COR) with detection at 700 nm. CHIP and UbcH5b∼Ub conjugate band intensities were quantitated using *Image Studio* (LI-COR). For each sample, the UbcH5b∼Ub conjugate band intensity was compared to the intensity of full-length CHIP in the same sample. UbcH5b∼Ub conjugate and CHIP band intensities were calibrated against inputs of known quantity. Calibration and data plotting were perfomed with *Prism* (GraphPad).

Cα−Cα Molecular Contact and Sanson−Flamsteed Orientation Plots. Cα−Cα contact distance plots for intra- and intermolecular interactions between E2 and Ub chains were calculated for PDB entries 3ugb (UbcH5c∼Ub), 3a33 (UbcH5b∼Ub), 3jw0 (UbcH5b∼Ub in complex with the NEDD4L-HECT), 2gmi (Ubc13∼Ub in complex with Mms2), 1fxt (Ubc1∼Ub), 2kjh (UbcH8−S−S−Ub), and 2fuh (UbcH5b·Ub noncovalent complex). For the NMR structures of PDB entries 2fuh, 2kjh, and 1fxt, the lowest-energy conformer was selected for all analyses. Contact distance plots were calculated using the Bio.PDB module within *BioPython*.[42] Briefly, Cα−Cα distance matrices were generated for select E2 and Ub pairs within each PDB file. These distance matrices were then plotted as a heat map using *matplotlib*[43] with a distance cutoff of 15 Å.

Sanson−Flamsteed plots were calculated using the Bio.PDB module within *BioPython* and the basemap toolkit within *matplotlib*. Briefly, the centers of mass (COMs) for the E2-conjugated ubiquitin chains in PDB entries 3ugb, 3a33, 3jw0, 2gmi, 1fxt, and 2kjh were calculated using the Bio.PDB module. A vector between each Ub COM and the Ub-conjugated serine OG or cysteine SG atom on the respective E2 was calculated using numerical python (*numpy*). The E2 OG−Ub COM vector was converted into spherical polar coordinates using *numpy* and plotted as a Sanson−Flamsteed projection plot using the basemap toolkit within *matplotlib*. Sanson−Flamsteed plots for conformers within UbcH5c∼Ub and Ubc13∼Ub SAXS ensembles were calculated in an identical fashion.

Ub Hot Spot Analysis. Cα−Cα distance matrices generated for each E2∼Ub structure using *BioPython* were utilized to identify the residues most commonly used by Ub to bind E2 through intraconjugate interactions. A Ub hot spot score was calculated following the procedure described by Winget and Mayor.[44] For every Ub residue within each E2∼Ub structure, the minimal distance to the E2 was calculated. The numbers of occurrences of minimal Cα−Cα distances of <10 Å were summed across all E2∼Ub structures, yielding the hot spot score (Figure S1 of the Supporting Information). Coloring of the hot spot score was scaled on the basis of the number of interactions for a given residue.

RESULTS

X-ray Crystal Structure of the Oxyester-Linked UbcH5c∼Ub Conjugate. We determined the structure of the oxyester-linked UbcH5c∼Ub conjugate by X-ray crystallography in space group $P12_11$ at 2.35 Å resolution (Table 1 and Figure 1A). A simulated annealing omit map confirms the correct placement of the covalent linkage between the UbcH5c Ser85 side chain hydroxyl oxygen and the C-terminal Ub Gly76 carbonyl carbon (Figure 1B). Electron density within a $2F_o - F_c$ map clearly identifies the UbcH5c∼Ub oxyester linkage and surrounding active site residues and bound water molecules (Figure S2 of the Supporting Information). Residues surrounding the UbcH5c active site, including the conserved Asp117 and Asn77, are poised to stabilize the C-terminus of Ub (Figure 1C). UbcH5c Asn77 does not contact the C-terminus of Ub directly but rather provides a key pair of hydrogen bonds that stabilize the UbcH5c Asp117-Pro118 loop. In contrast, the UbcH5c Asp117 side chain interacts directly with the C-terminus of Ub via a water-mediated hydrogen bond network. In addition to interactions between the UbcH5c active site and the C-terminus of Ub, intraconjugate contacts between Ub and UbcH5c are mediated by UbcH5c helix α3 residues Pro121, Glu122, and Arg125 and Ub α1−β3 loop residues Glu34, Gly35, Ile36, and Gln40 (Figure 1D).

Orientation of Ubiquitin in Structures of the E2∼Ub Conjugate. The orientation of Ub within E2∼Ub conjugates was previously examined by SAXS and NMR analyses of structures of Ubc13∼Ub and UbcH5c∼Ub conjugates in solution.[24] These analyses demonstrated that only a continuum of models, varying among "closed", "open", and "backbent" states, satisfies the SAXS and NMR data for these conjugates. The closed state is defined as an orientation in which the Ub is positioned against E2 crossover helix α2 (see Figure 1A for secondary structure labeling of E2 enzymes and Ub). In contrast, the open state places Ub below the E2 active site in a position with limited E2−Ub contacts. The structure of the UbcH5c∼Ub conjugate presented here (PDB entry 3ugb) and the two crystal structures of the UbcH5b∼Ub conjugate (PDB entries 3jw0 and 3a33) provide crystallographic evidence for backbent (PDB entries 3a33 and 3ugb) and open (PDB entry 3jw0) states (Figure 2A). The backbent state is defined as an orientation that folds the Ub "backward" against E2 loop 2, 4, 5, or 6. Currently, the UbcH5 subfamily (UbcH5a, UbcH5b, and UbcH5c, with sequences that are 88% identical and 98% similar) is the only E2 for which multiple E2∼Ub conjugate

Table 1. Crystallographic Data Collection and Refinement Statistics

	HsUbcH5c(1−147)(C85S)~HsUb(1−76)
Data Collection[a]	
X-ray source	Rigaku MicroMax-007HF
wavelength (Å)	1.5418
space group	$P12_11$
cell dimensions	
a, *b*, *c* (Å)	42.0, 52.5, 53.1
α, *β*, *γ* (deg)	90, 101.1, 90
resolution (Å)	52.51−2.35 (2.43−2.35)
R_{merge}[b]	0.048 (0.204)
R_{rim}[c]	0.053 (0.239)
$\langle I/\sigma I\rangle$[d]	19.2 (5.0)
Wilson *B* factor (Å^2)	41.3
completeness (%)	97.1 (78.2)
redundancy	4.9 (3.1)
no. of reflections	45575
no. of unique reflections	9319
Refinement	
resolution (Å)	29.57−2.35
no. of reflections for refinement	9298
R_{work}/R_{free}	0.211/0.253
no. of atoms	
protein	1766
water	128
glycerol	12
average *B* factor	
protein	45.3
water	46.1
glycerol	60.0
root-mean-square deviation	
bond lengths (Å)	0.014
bond angles (deg)	1.071
Ramachandran plot statistics (%)	
favored regions	98.2 (214/218)
allowed regions	100.0 (218/218)
disallowed regions	0.0
MolProbity validation statistics	
poor rotamers (%)	0.0
C*β* deviations >0.25 Å	0
clash score	16.55
clash percentile	76th percentile (*N* = 335, 2.35 ± 0.25 Å)
score	1.72
score percentile	98th percentile (*N* = 9377, 2.35 ± 0.25 Å)
PDB entry	3ugb

[a]Values in parentheses are for the highest-resolution shell. [b]The merging *R* factor is defined as $R_{merge} = [\sum_{hkl}\sum_i|I_i(hkl) - \overline{I(hkl)}|]/[\sum_{hkl}\sum_i I_i(hkl)]$. [c]The redundancy-indpendent merging *R* factor[65] is defined as $R_{rim} = (\sum_{hkl}\{[N/(N-1)]\}^{1/2}\sum_i|I_i(hkl) - \overline{I(hkl)}|)/[\sum_{hkl}\sum_i I_i(hkl)]$. [d]$\langle I/\sigma I\rangle$ denotes the averaged signal-to-noise ratio.

structures are deposited in the PDB. The other structures of the Ubc13~Ub (PDB entry 2gmi), Ubc1~Ub (PDB entry 1fxt), and UbcH8−S−S−Ub (PDB entry 2kjh) conjugates correspond to closed (PDB entry 1fxt) and backbent (PDB entries 2gmi and 2kjh) states, respectively (Figure 2B−D). In addition, a model of the Ube2s~Ub conjugate was reported[45] that places the Ub in the closed state (Figure S3 of the Supporting Information), similar to that of the Ubc1~Ub conjugate (PDB entry 1fxt).

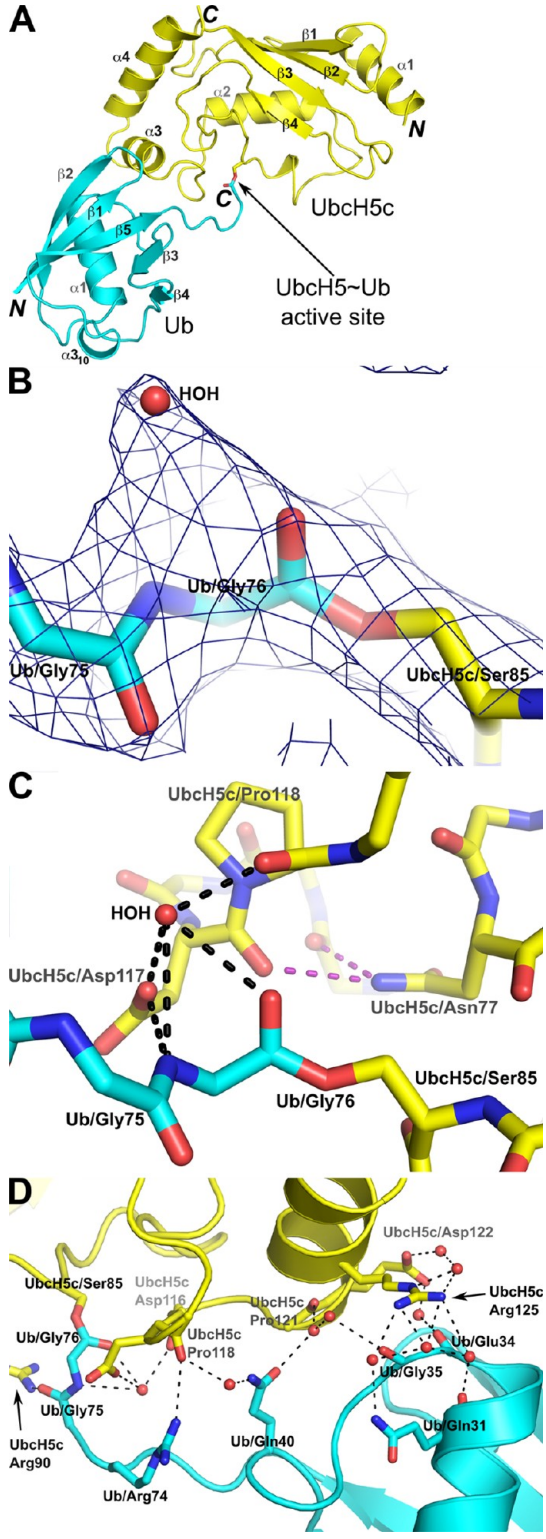

Figure 1. Structure of the UbcH5c~Ub conjugate. (A) Cartoon representation of the UbcH5c~Ub conjugate. The amino and carboxy termini of UbcH5c (yellow) and Ub (cyan) are labeled N and C, respectively. Secondary structure elements of UbcH5c and Ub are labeled *α* or *β*. (B) Close-up highlighting the oxyester bond between UbcH5c Ser85 and Ub Gly76. Water molecules are shown as red spheres, and the electron density for a simulated annealing omit map (dark blue) is contoured at 1*σ*. (C) C-Terminal tail of Ub participating in a water-mediated hydrogen bond network (black dashes) with the UbcH5c Asp117 side chain and UbcH5c Pro118 backbone. UbcH5c Asn77 provides supporting hydrogen bonds (purple dashes) that

dx.doi.org/10.1021/bi300058m | *Biochemistry* 2012, 51, 4175−4187

Figure 1. continued

stabilize the UbcH5c Asp117-Pro118 loop. For the sake of clarity, the hydrogen-bonded water molecule is labeled "HOH" and only the side chains of UbcH5c Asn77, UbcH5c Ser85, UbcH5c Asp117, and UbcH5c Pro118 are shown. (D) Intraconjugate contacts between UbcH5c and Ub utilize a water-mediated hydrogen bond network involving residues UbcH5c Pro121, UbcH5c Glu122, UbcH5c Arg125, Ub Glu34, Ub Gly35, and Ub Gln40.

Sanson–Flamsteed plots have been used to describe tensor orientations for NMR residual dipolar couplings[46,47] and tilt axis orientations in electron microscopy.[48] We used a Sanson–Flamsteed plot of the Ub center of mass with respect to the E2 active site to compare the relative orientations of Ub in different conjugate structures (Figure 2E). Although no two E2~Ub conjugate structures have identical Ub positions, some commonalities are present. PDB entries 3ugb and 2kjh (backbent state) and PDB entry 1fxt and the Ube2s~Ub conjugate (closed state) (Figure 2E and Figure S3 of the Supporting Information) exhibit the most similar relative Ub orientations. Furthermore, the Sanson–Flamsteed plot clearly delineates the difference between solution phase SAXS ensembles for UbcH5c~Ub (Figure 2F) and Ubc13~Ub

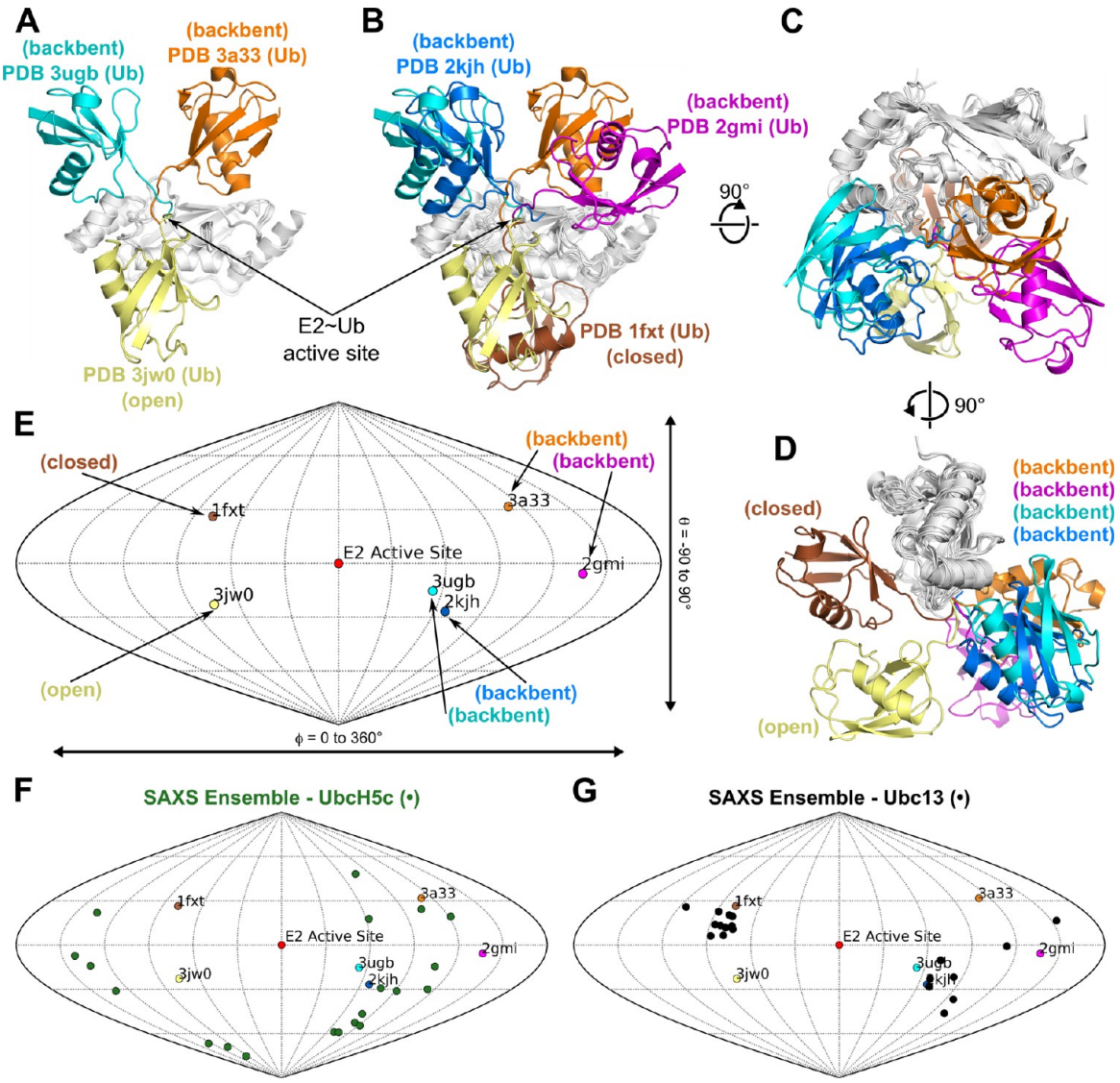

Figure 2. Relative orientations of known E2~Ub conjugate structures in the PDB. (A) Three distinct Ub positions within structures of UbcH5~Ub conjugates: PDB entry 3ugb for UbcH5c~Ub (Ub, cyan; UbcH5c, gray), PDB entry 3a33 for UbcH5b~Ub (Ub, orange; UbcH5c, gray), and PDB entry 3jw0 for UbcH5b~Ub (Ub, yellow; UbcH5b, gray). An arrow denotes the location of the E2~Ub active site. (B) Structures of E2~Ub conjugates exhibit a range of Ub positions: PDB entry 3ugb for UbcH5c~Ub (Ub, cyan; UbcH5c, gray), PDB entry 3a33 for UbcH5b~Ub (Ub, orange; UbcH5c, gray), PDB entry 3jw0 for UbcH5b~Ub (Ub, yellow; UbcH5b, gray), PDB entry 2gmi for Ubc13~Ub (Ub, magenta; Ubc13, gray), PDB entry 1fxt for Ubc1~Ub (Ub, brown; Ubc1, gray), and PDB entry 2kjh for UbcH8–S–S–Ub (Ub, blue; UbcH8, gray). (C) Ninety degree rotation of panel B about the *x*-axis. (D) Ninety degree rotation of panel C about the *y*-axis. (E) Sanson–Flamsteed plot corresponding to the structural overlay in panel D indicating the orientation of the Ub center of mass with respect to the E2 active site Ser OG or Cys SG atom in PDB entries 1fxt (brown), 2gmi (magenta), 2kjh (blue), 3a33 (orange), 3jw0 (yellow), and 3ugb (cyan). (F) Sanson–Flamsteed plot from panel E with the 20 members of the UbcH5c~Ub SAXS ensemble (green).[24] (G) Sanson–Flamsteed plot from panel E with the 20 members of the Ubc13~Ub SAXS ensemble (black).[24]

dx.doi.org/10.1021/bi300058m | *Biochemistry* 2012, 51, 4175–4187

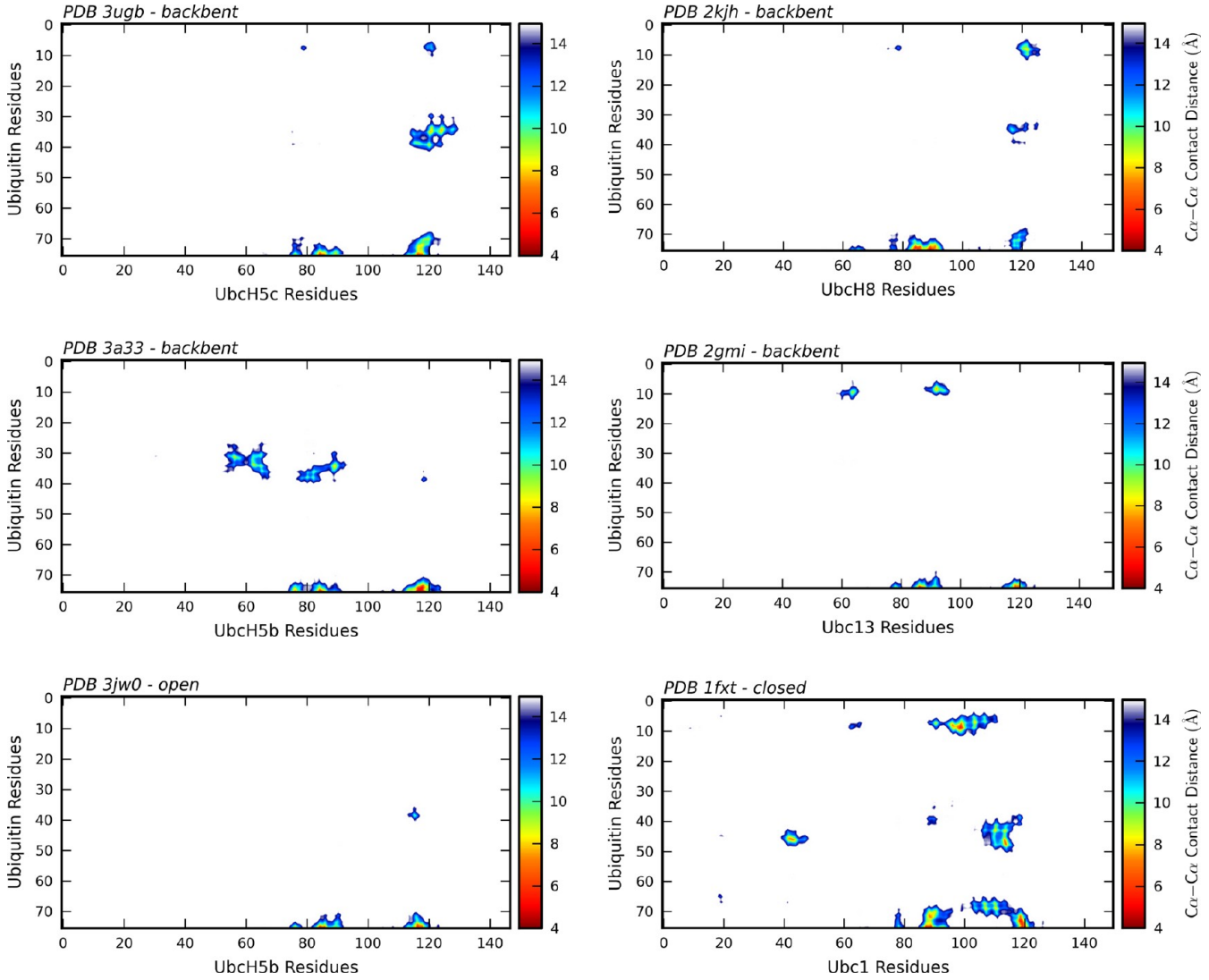

Figure 3. Intraconjugate Cα−Cα contact distance plots. Cα−Cα intraconjugate contact distance plots for PDB entries 3ugb (UbcH5c∼Ub), 3a33 (UbcH5b∼Ub), 3jw0 (UbcH5b∼Ub with NEDD4L-HECT), 2gmi (Ubc13∼Ub with Mms2), 2kjh (UbcH8−S−S−Ub), and 1fxt (Ubc1∼Ub) indicate E2∼Ub residue pairs separated by a distance of ≤15 Å. For each structure, Ub residues are shown on the *y*-axis and E2 residues are shown on the *x*-axis. A color bar associated with each plot indicates the Cα−Cα contact distance.

(Figure 2G) conjugates. While members of the UbcH5c SAXS ensemble occupy a range of Ub positions, members of the Ubc13 ensemble form discrete clusters matching the closed and backbent states.

Interestingly, the relative orientation of Ub does not correlate with the solvent accessible surface area (SASA) of the E2∼Ub active site ester bond (Table S1 of the Supporting Information) calculated with *WHATIF*.[49] For example, of the four backbent state structures (PDB entries 2gmi, 2kjh, 3a33, and 3ugb), three can be classified as accessible (2gmi, 2kjh, and 3a33) while the fourth is more occluded (3ugb). The average active site SASA of the backbent state accessible structures is 12.86 Å^2 compared to 6.26 Å^2 for the single backbent state occluded structure. Furthermore, the active site SASA values for the two closed structures (PDB entry 1fxt and Ube2s∼Ub) are markedly different. The active site SASA is 11.40 Å^2 in PDB entry 1fxt but only 6.13 Å^2 for Ube2s∼Ub. The active site SASA for PDB entry 3jw0, the only open state structure, is 5.37 Å^2, within 1 Å^2 of that of the occluded backbent state structure of PDB entry 3ugb and the occluded closed state model Ube2s∼Ub. These results suggest that Ub orientation does not directly dictate the accessibility of the E2∼Ub thioester bond.

Specific Interactions Potentiate Ub Orientations. An examination of all six E2∼Ub structures using Cα−Cα contact distance plots allows for rapid identification of specific interactions between the E2 and Ub (Figure 3). Although all E2∼Ub structures exhibit close contacts between the C-terminus of Ub and the E2 active site, each structure also contains additional interactions. An initial analysis of Cα−Cα contact distance plots reveals commonalities that group the structures into four distinct groups.

Interactions between Ub residues 8−10 and 35−40 and helix α3 of E2 characterize the first group, comprised of PDB entries 3ugb (UbcH5c∼Ub) and 2kjh (UbcH8−S−S−Ub). The primary difference between the two structures is a slight relative rotation that places the β1−β2 loop of Ub closer to the E2 in PDB entry 2kjh, while the α1−β3 loop of Ub is closer in PDB entry 3ugb. Both PDB entries 2kjh and 3ugb are examples of the backbent state. The second group includes PDB entries 2gmi (Ubc13∼Ub with Mms2) and 3a33 (UbcH5b∼Ub),

dx.doi.org/10.1021/bi300058m | *Biochemistry* 2012, 51, 4175−4187

which represent variations on the backbent state. Although the orientations of Ub are different for PDB entries 2gmi and 3a33, the E2 interaction surface is nearly identical, with interactions limited to the E2 active site and the $\beta3-\beta4$ loop of E2.

The third group contains a single member, PDB entry 3jw0 (UbcH5b∼Ub with NEDD4L-HECT). Although the UbcH5∼Ub complex prefers the open state in solution,[24] the only crystal structure in an open state is that of the UbcH5b∼Ub complex with NEDD4L-HECT (PDB entry 3jw0), in which the extended position of the Ub is stabilized by interactions with NEDD4L-HECT. In the absence of a third protein (the HECT domain), such an extended conjugate structure would not form a stable crystal lattice. The C$\alpha-$Cα contact distance plot of PDB entry 3jw0 (Figure 3) shows the limited nature of E2−Ub contacts for this open state structure. The C$\alpha-$Cα contact distance plot of PDB entry 3jw0 indicates residues 39 and 40 near the beginning of Ub strand $\beta3$ that most closely approach E2. Interestingly, these residues are also involved in E2−Ub contacts in the UbcH5c∼Ub (PDB entry 3ugb) and UbcH5b∼Ub (PDB entry 3a33) backbent structures.

The single member of the fourth group, PDB entry 1fxt (Ubc1∼Ub), is the only closed state structure in the PDB. Intermolecular contacts in this structure and in the Ube2s∼Ub model (Figure S3 of the Supporting Information) are primarily mediated by the hydrophobic face of Ub Ile44. Although these contacts are unique to the closed state, other E2−Ub contacts involving residues in the $\beta1-\beta2$ loop of Ub are similar to those in the backbent state structures of PDB entries 2gmi (Ubc13∼Ub) and 2kjh (UbcH8−S−S−Ub).

The patterns of C$\alpha-$Cα contacts across different E2 enzymes and variable intraconjugate relative Ub orientations indicate that a relatively limited subset of Ub residues mediate interaction with the E2. To highlight the key interacting residues, we converted the E2∼Ub C$\alpha-$Cα contact distance plots (Figure 3) into a Ub hot spot score, following the protocol of Winget and Mayor.[44] A heat map produced from the Ub hot spot score was used to color residues of Ub (Figure 4 A,B and Figure S1 of the Supporting Information). Residues 8−11, 36, 39, 71, and 73−76 are the Ub epitopes most commonly involved in intraconjugate interactions. These residues map to a single face of Ub formed by loops 1 and 3 and the C-terminal tail. A closer examination of the E2∼Ub structures emphasizes that each E2∼Ub structure uses nearly the same face of Ub to interact with the E2.

UbcH5 and the Backside Interaction. The UbcH5·Ub backside interaction was first reported by Brzovic et al.[25] The NMR structure of the noncovalent UbcH5c·Ub complex (PDB entry 2fuh) identified intimate contacts between the β-sheet of UbcH5c and the hydrophobic face of Ub Ile44 and the $\beta4-\alpha3_{10}$ loop (Figure 5A). E2·Ub backside interactions are present in models of noncovalent Ube2g2·Ub and Ubc2b·Ub complexes[50,51] and in a crystal structure of a noncovalent (unconjugated) UbcH5a·Ub complex (PDB entry 3ptf).[52] Backside-mediated contacts have also been observed between the E2 Ubc9 and the small ubiquitin-like modifier (SUMO).[26,29] The first example of the backside interaction in the context of E2∼Ub conjugates was observed in the crystal structure of the UbcH5b∼Ub conjugate in space group $P6_122$ (PDB entry 3a33).[21] Our new structure of the UbcH5c∼Ub conjugate in space group $P12_11$ provides additional crystallographic evidence of the backside interaction in an E2∼Ub conjugate (Figure 5A). C$\alpha-$Cα contact distance plots for the

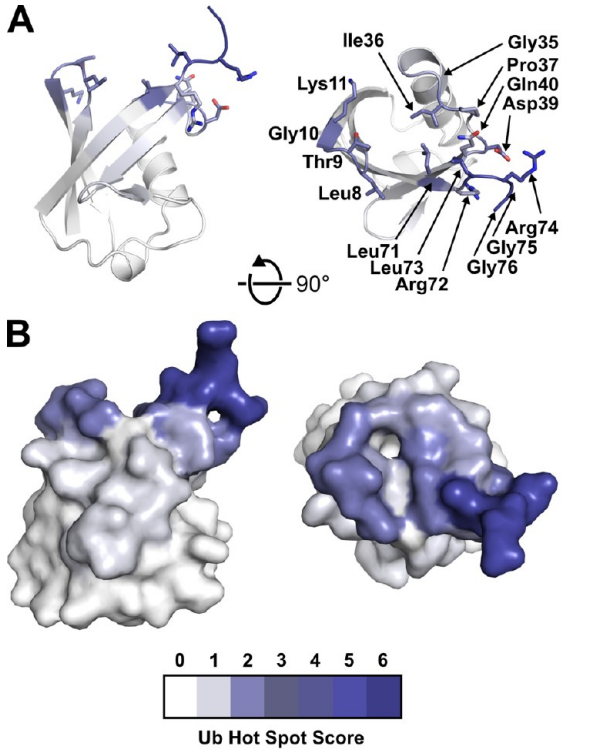

Figure 4. Ubiquitin intraconjugate E2 interaction hot spot mapping. (A) Cartoon representation of Ub residues (PDB entry 1ubq) colored by the Ub hot spot score as determined according to the degree of participation in intraconjugate interaction with the E2 for PDB entries 1fxt, 2gmi, 2kjh, 3a33, 3jw0, and 3ugb. The side chain atoms of residues most commonly participating in intraconjugate interactions with the E2 are shown as sticks. (B) Surface representation of panel A. A color bar indicates coloring used to represent the hot spot score in panels A and B.

UbcH5·Ub backside interaction within both UbcH5∼Ub structures demonstrate that each structure utilizes a nearly identical pattern of E2·Ub contacts (Figure S4 of the Supporting Information).

Structural Variability and Diversity in UbcH5∼Ub Conjugate Oligomerization. Extensive line broadening observed in NMR spectra of UbcH5∼Ub conjugates[25] suggested that the UbcH5·Ub backside interaction causes UbcH5∼Ub conjugates to form higher-order oligomers. The first crystal structure of an oligomerized conjugate (UbcH5b∼Ub)[21] revealed an infinite spiral oligomer (Figure 5B). The structure presented here (PDB entry 3ugb) demonstrates a second architecture for UbcH5∼Ub oligomers, in which the Ub orientation results in a staggered linear array oligomer (Figure 5C). The UbcH5∼Ub structures of PDB entries 3a33 and 3ugb demonstrate that the UbcH5·Ub backside interaction is compatible with multiple relative Ub orientations. Additionally, the positions of UbcH5 molecules within the staggered linear array result in E2·E2 interactions (Figure 5D). Such interactions were predicted in the original UbcH5∼Ub backside interaction study[25] but are not present in the infinite spiral oligomer (PDB entry 3a33). The E2·E2 interaction surface within the staggered linear array comprises a surface area of 330 Å^2 as calculated with *PISA*.[53] The interactions at this E2·E2 interface include a water-mediated hydrogen bond network, a salt bridge between Glu140 and Lys66, and a cation$-\pi$ interaction between Arg136 and His55 (Figure 5D). Despite

dx.doi.org/10.1021/bi300058m | *Biochemistry* 2012, 51, 4175−4187

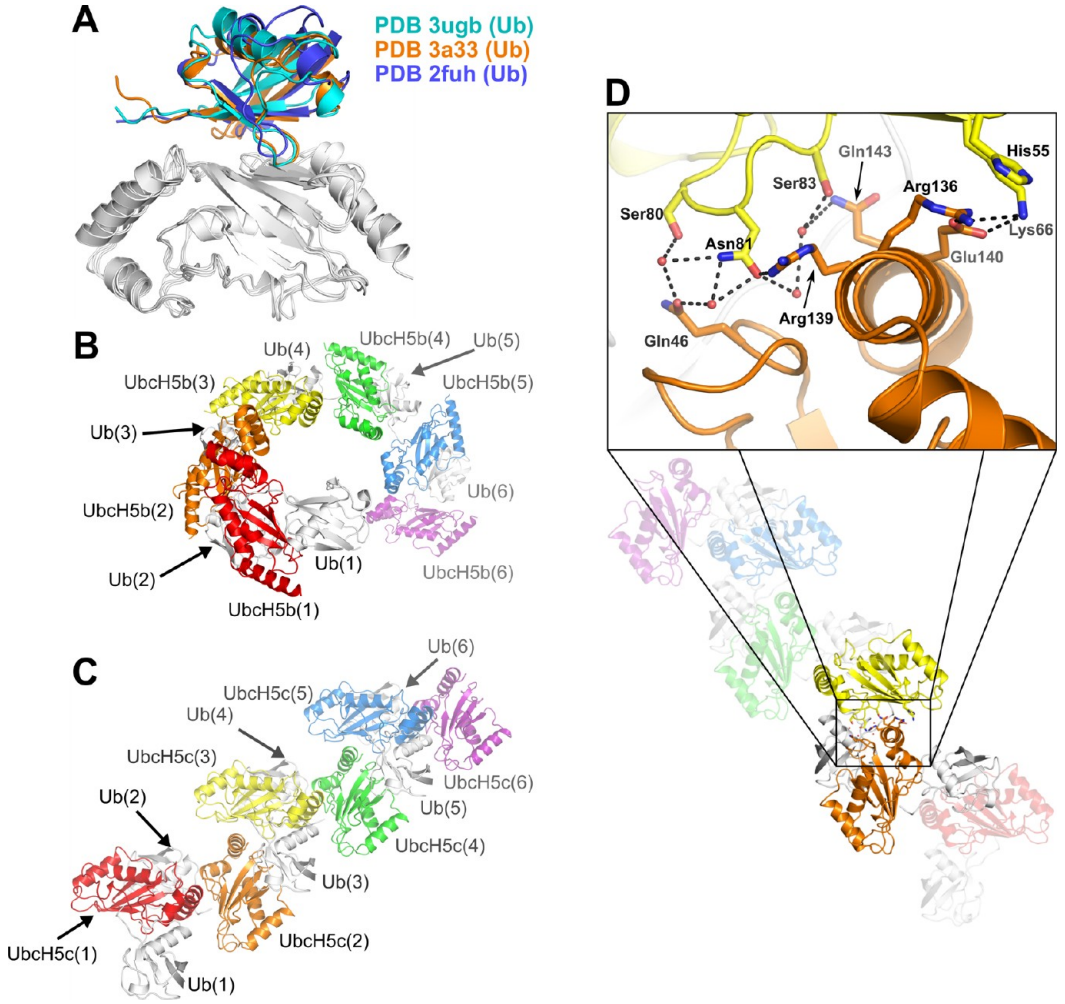

Figure 5. Canonical UbcH5·Ub backside interaction and relative intraconjugate Ub orientation determine the geometry of UbcH5∼Ub oligomers. (A) The positions of ubiquitin chains participating in a backside interaction with UbcH5 (white) are nearly identical for PDB entries 3ugb (cyan), 3a33 (orange), and 2fuh (blue). (B) The relative orientations of UbcH5b and Ub in PDB entry 3a33 in combination with the UbcH5·Ub backside interaction produce an infinite spiral of UbcH5b∼Ub molecules. (C) The relative orientations of UbcH5c and Ub in PDB entry 3ugb in combination with the UbcH5·Ub backside interaction create an infinite staggered linear array of UbcH5c∼Ub molecules. (D) Residues mediating contacts between UbcH5c molecules from neighboring conjugates in the staggered linear array are shown as sticks. Water molecules are shown as red spheres. Hydrogen bonds and salt bridges are shown as dashed lines (black). For panels B–D, UbcH5 molecules are colored red, orange, yellow, green, blue, or purple and all Ub molecules are colored white.

the addition of the E2·E2 interface in the staggered linear UbcH5∼Ub oligomers, the two architectures result in similar total buried surface areas, because of the different orientations of Ub in the two oligomers. A staggered linear UbcH5c∼Ub dimer buries a surface area of 1725 Å^2, while an infinite spiral UbcH5b∼Ub dimer buries a surface area of 1700 Å^2.

E3 Ubiquitin Ligase CHIP Interacts with UbcH5∼Ub Conjugate Oligomers. Existing structures of UbcH5 in complex with both HECT- and RING/U-box-type E3 enzymes do not occlude the UbcH5 residues involved in backside-mediated oligomerization. While E3s should be able to bind directly to directly to such oligomers, this interaction has not been experimentally verified. We therefore performed pull-down assays with the U-box-type ligase CHIP and UbcH5b∼Ub conjugates. We first bound His$_6$-tagged CHIP to Ni-coated magnetic beads and probed them with increasing concentrations of the oligomerization deficient UbcH5b(C85S/S22R)∼Ub conjugate. The UbcH5b S22R mutation prevents backside-mediated oligomerization, resulting in a monomeric UbcH5∼Ub species, but does not perturb the interaction between CHIP and UbcH5b. The pull-down assays (Figure 6A) indicate that CHIP interacts with the monomeric conjugate in a saturable manner (Figure 6C). In contrast, CHIP pulls down a larger quantity of oligomerization-competent UbcH5b(C85S)∼Ub conjugate that increases linearly with the addition of the conjugate and does not become saturated within the range examined (Figure 6B). These results demonstrate that CHIP interacts directly with an oligomerized UbcH5∼Ub conjugate. In our experiment, on the basis of a comparison of the intensities of the respective UbcH5b(C85S)∼Ub and UbcH5b(C85S/S22R)∼Ub bands to the intensities of input controls (data not shown), each CHIP-bound conjugate oligomer is comprised of four UbcH5∼Ub conjugates on average. The trend seen in Figure 6C suggests that UbcH5∼Ub oligomers bound to CHIP may contain even higher numbers of conjugate molecules.

■ DISCUSSION

E2∼Ub conjugates play a central role in the ubiquitination cascade. The structure of the UbcH5c∼Ub conjugate adds to a

dx.doi.org/10.1021/bi300058m | *Biochemistry* 2012, 51, 4175–4187

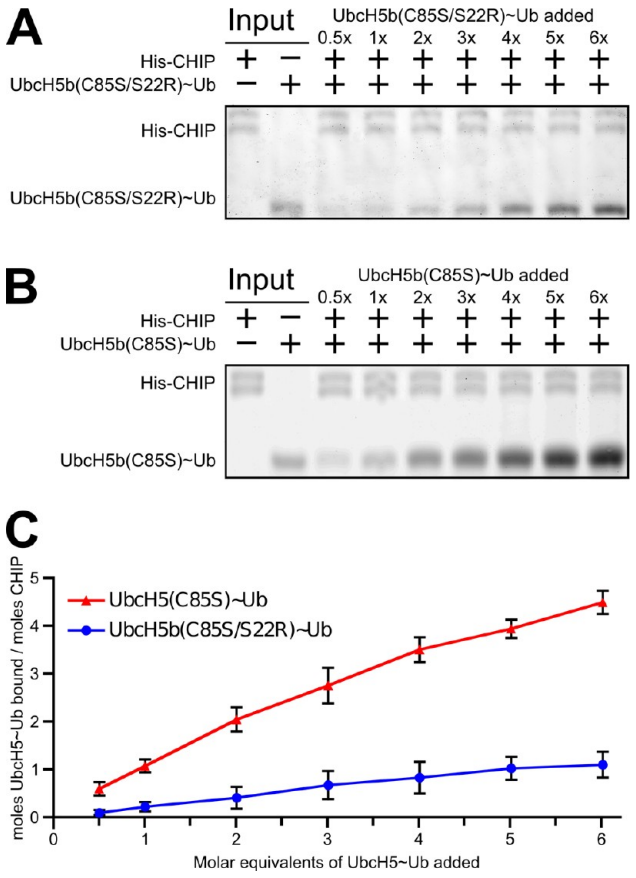

Figure 6. Interaction of UbcH5~Ub conjugate oligomers with the U-box-type E3 CHIP. (A) Full-length His_6-CHIP, bound to Ni-coated magnetic beads, was used to pull down the backside-mediated oligomerization deficient HsUbcH5b(C85S/S22R)~Ub conjugate (A) or the backside-mediated oligomerization competent HsUbcH5b-(C85S)~Ub conjugate (B) at the indicated molar equivalents. Eluted CHIP and UbcH5b~Ub conjugate in panels A and B were analyzed by SDS–PAGE. Gels were stained with IRDye Blue Protein Stain (LI-COR) and detected by fluorescence imaging at 700 nm. (C) LI-COR-quantified UbcH5~Ub band intensities were compared to the eluted CHIP intensity within the same lane, calibrated against input bands and plotted as a function of the number of molar equivalents of the UbcH5b~Ub conjugate added. Data points represent the average of three separate trials, with error bars indicating the standard deviation.

small but growing library of E2~Ub conjugate structures and allows for insights into the effect of Ub orientation on active site accessibility, organization, and intra- and interconjugate interactions. Here we find that UbcH5~Ub conjugates are not limited to the previously reported infinite spiral arrangement and can also adopt a linearly staggered arrangement. The UbcH5·Ub backside interaction is maintained in both oligomers and is not constrained by the variable intraconjugate Ub orientation.

Are extended oligomers that result from iteration of the UbcH5·Ub backside interaction compatible with E3 ubiquitin ligases? We found direct evidence of an interaction between a U-box-type E3 and UbcH5~Ub oligomers (Figure 6). We examined the compatibility of the two structurally characterized UbcH5~Ub conjugate oligomers with the UbcH5-interacting domains of representative E3 ubiquitin ligases. We docked both the staggered linear array and infinite spiral UbcH5~Ub oligomers onto U-box and HECT domains using the structure of UbcH5a in complex with the U-box domain of CHIP[32] and the structure of the UbcH5b~Ub conjugate in complex with the HECT domain of NEDD4L[20] (Figure S5 of the Supporting Information). The staggered linear array and infinite spiral UbcH5~Ub oligomers are tolerated in both docked models without any steric clashes. We extended the docking analysis by using the full-length structures of CHIP[54] and the Cul1-Rbx1-Skp1-Skp2 SCF ligase, a multisubunit RING-type ligase.[55] Both architectures are accommodated by full-length CHIP and SCF ligases without any steric clashes (Figure S6 of the Supporting Information). Both oligomers extend away from the E3s, and no E3·conjugate interactions are evident other than the E2·E3 interaction surface between the E3 RING/U-box domains and the "initiating" E2s of the oligomers that are present in the original crystal structures.

Throughout the staggered linear array and infinite spiral UbcH5~Ub oligomeric chains, the RING/U-box E3 binding site is unobstructed. The extended oligomers thus contain many potentially accessible RING/U-box E3 binding sites, suggesting that more than one E3 may bind to a UbcH5~Ub oligomeric assembly. While our pull-down experiment does not allow us to distinguish between this possibility and the possibility that the E3 binds only to the initiating conjugate in the oligomer, a closer examination of modeled E3·Ub-cH5~Ub complexes (Figures S5 and S6 of the Supporting Information) provides insight. HECT domains bind Ub in an orientation that does not allow for a simultaneous backside interaction, as the noncovalently interacting E2 would clash with the HECT domain. Most likely, HECT-type ligases therefore bind only to the initiating conjugate. Such a steric restriction does not apply to the CHIP or SCF ligases, suggesting that these RING/U-box E3s are able to bind at multiple sites along an oligomer. However, Deshaies and co-workers showed that formation of a transient closed state is required for E3-mediated ubiquitination by the E2 enzyme Cdc34, and likely also by UbcH5.[56] In the closed state, the canonical Ub Ile44 binding surface is occluded by the E2 and cannot participate in the backside interaction. However, the E2 backside binding surface of a closed state conjugate is unobstructed and competent for binding ubiquitin. This suggests that the closed state could be allowed for the initiating conjugate but not for other conjugates in the oligomer. Thus, if ubiquitination is to proceed, the mechanistic requirement of a closed state Ub orientation may limit RING/U-box E3s to binding only the initiating conjugate.

Solution phase studies indicate that the Ub orientation is dynamic,[24,51] implying that UbcH5~Ub oligomers might also be dynamic. Models of CHIP and SCF ligases in complex with UbcH5~Ub oligomers (Figure S6 of the Supporting Information) suggest that a wide range of conformationally dynamic UbcH5~Ub oligomers are accommodated by RING/U-box E3 ubiquitin ligases. The range of possible UbcH5~Ub oligomers can be represented by combining the UbcH5·Ub backside interaction with intraconjugate Ub orientations that are compatible with UbcH5~Ub oligomerization. Unlike the closed state, open and backbent state Ub orientations are compatible with the UbcH5~Ub backside interaction and could occur anywhere within an E2~Ub conjugate oligomer. Combinations of UbcH5~Ub conjugates with intraconjugate Ub orientations from the UbcH5b~Ub (PDB entry 3a33) and UbcH5c~Ub (PDB entry 3ugb) structures could produce many distinct oligomers (Figure S7A of the Supporting Information). For example, a chain assembly of four UbcH5~Ub conjugates utilizing the two Ub orientations

dx.doi.org/10.1021/bi300058m | *Biochemistry* 2012, 51, 4175–4187

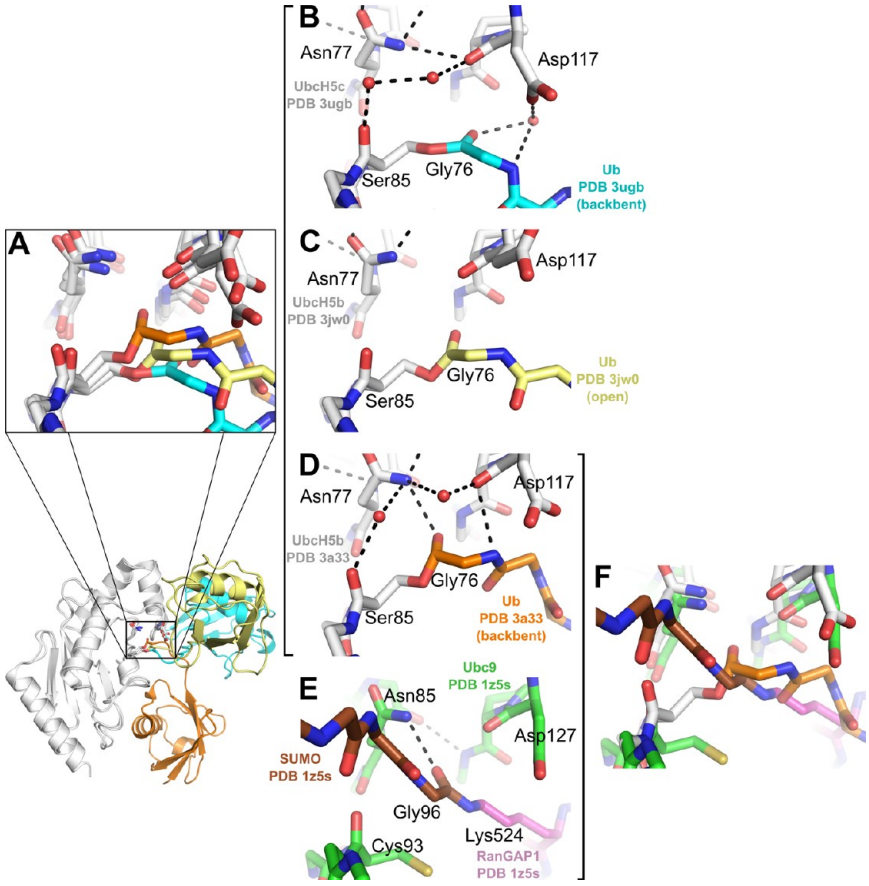

Figure 7. Comparison of molecular environments surrounding the active site of the E2∼Ub conjugate. (A) Comparison of E2∼Ub active site environments for PDB entries 3ugb (UbcH5c, white; Ub, cyan), 3a33 (UbcH5b, white; Ub, orange),[21] and 3jw0 (UbcH5b, white; Ub, yellow).[20] A zoomed-out cartoon view highlights the location of the E2∼Ub active site. (B) E2∼Ub active site environment for PDB entry 3ugb (UbcH5c, white; Ub, cyan). (C) E2∼Ub active site environment for PDB entry 3jw0 (UbcH5b, white; Ub, yellow). (D) E2∼Ub active site environment for PDB entry 3a33 (UbcH5b, white; Ub, orange). (E) E2∼Ub active site environment for PDB entry 1z5s (Ubc9, green; SUMO, brown; RanGAP1, purple).[61] (F) Comparison of E2∼Ub active site environments for PDB entries 3a33 (UbcH5b, white; Ub, orange) and 1z5s (Ubc9, green; SUMO, brown; RanGAP1, purple).

from PDB entries 3a33 and 3ugb could form eight (2^3) different isomers. However, the topology of conjugate oligomers is likely even less constrained than that suggested by the two current oligomeric crystal structures. An ensemble of 20 E2∼Ub orientations was required to fully reproduce the experimental SAXS curve for the UbcH5c∼Ub conjugate.[24] If we limit the available UbcH5∼Ub orientations to those found in current E2∼Ub structures that are compatible with backside-mediated oligomerization (five structures, PDB entries 2gmi, 2kjh, 3a33, 3jw0, and 3ugb), an oligomer comprised of four UbcH5∼Ub conjugates could form as many as 125 (5^3) different isomers (Figure S7B−F of the Supporting Information). The diversity of possible E2∼Ub oligomer topologies, in combination with the conformational dynamics observed by SAXS and NMR, suggests that that UbcH5∼Ub oligomers are likely to be conformationally diverse and dynamic. While the staggered linear array and infinite spiral architectures are currently the only structurally characterized UbcH5∼Ub oligomers, these architectures probably represent only two of many UbcH5∼Ub conjugate oligomers.

The continuum of transiently occupied open, closed, and backbent states identified by SAXS and NMR analyses[24] and by the E2∼Ub structures discussed here may have important functional consequences apart from their effects on oligomerization. For one, with the exception of the closed state model of PDB entry 1fxt (Ubc1∼Ub), it is significant that none of the structures utilize the canonical recognition surface of Ub Ile44 for intraconjugate interactions. The I44 surface is engaged by the majority of known ubiquitin-binding domains.[57] The use of a noncanonical Ub recognition surface could allow the exposed surface of Ub Ile44 to participate in additional interactions in larger ternary complexes, such as those suggested by models of the interactions among Ub, the ZNF216 A20-like zinc finger ubiquitin binding domain, and the ubiquitin-associated (UBA) domain of p62.[58] Additionally, exposure of the surface of Ub Ile44 in an E2∼Ub conjugate would allow for engagement with ubiquitin binding domains on proteins that undergo self-ubiquitination even in the absence of E3s.[59]

The transiently occupied states of the conjugate may also have more direct implications for catalysis and ubiquitin transfer. Our comparison of active site SASA suggests that the relative orientation of Ub does not dictate the accessibility of the active site thioester bond. However, solvent accessibility is not the sole requirement for active site competency. Previous studies have shown that both a conserved asparagine (UbcH5 Asn77)[60] and a conserved aspartate (UbcH5 Asp117)[7,60] play critical roles in the transfer of Ub to lysines. Although the specific roles of these two residues remain to be experimentally confirmed, it has been proposed that that UbcH5 Asn77 stabilizes the oxyanion and hydrogen bonds to the Ub Gly76

dx.doi.org/10.1021/bi300058m | *Biochemistry* 2012, 51, 4175−4187

carbonyl prior to Ub transfer, while UbcH5 Asp117 is thought to act as a general base, both deprotonating and lowering the pK_a of the incoming lysine. Interestingly, the positions and orientations of the Ub backbone at the thioester and the key active site residues UbcH5 Asn77, UbcH5 Asp117, and UbcH5 Ser85 (Figure 7A) differ in the three available UbcH5~Ub structures (PDB entries 3a33, 3jw0, and 3ugb).

In our UbcH5c~Ub structure [PDB entry 3ugb (Figure 7B)], the Ub backbone participates in a water-mediated hydrogen bond to the side chain of UbcH5 Asp117. UbcH5 Asn77 stabilizes the UbcH5 Asp117-Pro118 loop and is not in position to form a hydrogen bond with the carbonyl of Ub Gly76. UbcH5 Asn77-mediated stabilization of the Asp117-Pro118 loop is observed in both PDB entries 3ugb (UbcH5c~Ub) and 2gmi (Ubc13~Ub with Mms2). In contrast, the UbcH5b~Ub structure in complex with NEDD4L-HECT exhibits a different active site organization. In this structure [PDB entry 3jw0 (Figure 7C)], UbcH5 Asp117 is disengaged from the Ub backbone, allowing rotation of the Ub backbone toward UbcH5 Asn77. The UbcH5b~Ub structure [PDB entry 3a33 (Figure 7D)] presents a third, distinct active site organization. In this structure, the backbone carbonyl of Ub Gly76 is hydrogen-bonded to the side chain of UbcH5 Asn77, a position that may allow UbcH5 Asn77 to stabilize the oxyanion upon attack by a lysine. Furthermore, UbcH5 Asp117 does not interact with the C-terminus of Ub but may be poised for interaction with an incoming lysine. While there are no transition state structures, or post-Ub transfer structures for the UbcH5−Ub system, a structure of Ubc9 in complex with SUMOylated RanGAP1[61] (Figure 7E) provides clues about the organization of the E2 active site after Ub transfer. Intriguingly, the active site organizations for the UbcH5b~Ub structure (PDB entry 3a33) and the Ubc9·RanGAP1~SUMO complex (PDB entry 1z5s) are remarkably similar (Figure 7F). In both structures, Ub Gly76 (SUMO Gly96) is in position to interact with the side chain of E2 Asn77. Additionally, the position of the side chain of E2 Asp117 is similarly disengaged from the Ub or SUMO backbone in both structures.

The difference in active site orientations among the UbcH5~Ub structures thus raises an interesting question. What is the relationship among relative Ub orientation, active site organization, and active site activation? Although the closed state Ub orientation has been shown to be important for activating Ub transfer by aminolysis,[56] the absence of a UbcH5~Ub or E2~Ub closed state structure in which side chain orientations have been explicitly determined prevents a direct comparison to the existing UbcH5~Ub structures. The relationship between E2~Ub active site organization and Ub orientation may be important for E2 enzymes that interact with different families of E3 enzymes. For example, the UbcH5 family of E2 enzymes participates in Ub transfer with RING-, U-box-, and HECT-type E3s with widely divergent architectures. It is unlikely that interactions with RING/U-box-type versus HECT-type E3 enzymes result in identical or even similar relative Ub orientations. The E2~Ub active site must nevertheless be activated or made competent for activation, to allow for E3-mediated nucleophilic attack and ubiquitin transfer. The ability to tune the E2~Ub active site reactivity by altering Ub orientation may allow the E2~Ub conjugate to be competent for Ub transfer via aminolysis or transthiolation, depending upon the identity of the E3.

The number of E2~Ub conjugate structures deposited in the PDB is now beginning to reach a critical mass that allows for insights into the mechanisms underlying ubiquitination. Nevertheless, additional structures of E2~Ub conjugates are still needed. In particular, E2~Ub conjugate structures in complex with a range of E3 enzymes may show whether the mechanisms of ubiquitination are specific to each class of E3 enzymes or whether more general mechanisms exist. Furthermore, structures of E2~Ub conjugates from additional E2 families will shed light on the role of both intra- and interconjugate E2−Ub interactions. For the UbcH5 family of E2~Ub conjugates, transition state or pre- and post-transition state structures would contribute significantly to our understanding of the molecular mechanisms of ubiquitination. Although a transition state structure including the oxyanion intermediate poses a difficult challenge to structural biology, recent advances in synthetically modified Ub moieties[62−64] may provide potential avenues for approaching the characterization of pre- and post-transition state structures. While much work remains to be completed on the road to characterizing the mechanisms of E3-mediated ubiquitination, the structure of the UbcH5c~Ub conjugate presented here provides valuable insights into intraconjugate E2·Ub interactions, the organization of the E2~Ub active site, and the dynamic, versatile architecture of E2~Ub conjugate oligomers.

■ ASSOCIATED CONTENT

Supporting Information

Molecular modeling protocol for generating the Ube2s~Ub conjugate, Ube2s~Ub Cα−Cα contact plot, comparison of Ube2s~Ub and E2~Ub structures deposited in the PDB, sequence scoring chart for Ub hot spot analysis, $2F_o - F_c$ electron density map for the UbcH5c~Ub oxyester linkage, Cα−Cα contact plots and structural alignments of UbcH5·Ub structures deposited in the PDB that contain the backside interaction, modeled complexes between UbcH5~Ub oligomers and CHIP-U-box, NEDD4L-HECT, full-length CHIP, and Cul1-Rbx1-Skp1-Skp2 SCF ligases, and models of variable topology E2~Ub oligomers. This material is available free of charge via the Internet at http://pubs.acs.org.

■ AUTHOR INFORMATION

Corresponding Author

*Department of Molecular Cardiology, Lerner Research Institute, Cleveland Clinic NB20, 9500 Euclid Ave., Cleveland, OH 44195. Telephone: (216) 444-2054. Fax: (216) 445-8204. E-mail: pager2@ccf.org (R.C.P.) or misras@ccf.org (S.M.).

Author Contributions

R.C.P. and J.N.P. contributed equally to this work.

Funding

This work was supported by National Institutes of Health (Grant RO1-GM080271 to S.M. and Grant RO1-GM088055 to R.E.K.). R.C.P. was partly supported by Public Health Service (PHS) National Research Service Award (NRSA) Postdoctoral Fellowship T32 HL007914. J.N.P. was supported by PHS NRSA Predoctoral Fellowship T32 GM008268.

Notes

The authors declare no competing financial interest.

■ ABBREVIATIONS

CHIP, carboxyl terminus of Hsp70 interacting protein; E1, ubiquitin-activating enzyme; E2, ubiquitin-conjugating enzyme;

E3, ubiquitin ligase; HECT, homologous to the carboxy terminus of E6AP; NMR, nuclear magnetic resonance; RING, really interesting new gene; SAXS, small-angle X-ray scattering; Ub, ubiquitin.

REFERENCES

(1) Hershko, A., and Ciechanover, A. (1998) The ubiquitin system. *Annu. Rev. Biochem. 67*, 425−479.

(2) Pickart, C. M., and Fushman, D. (2004) Polyubiquitin chains: Polymeric protein signals. *Curr. Opin. Chem. Biol. 8*, 610−616.

(3) Pickart, C. M., and Eddins, M. J. (2004) Ubiquitin: Structures, functions, mechanisms. *Biochim. Biophys. Acta 1695*, 55−72.

(4) Cyr, D. M., Hohfeld, J., and Patterson, C. (2002) Protein quality control: U-box-containing E3 ubiquitin ligases join the fold. *Trends Biochem. Sci. 27*, 368−375.

(5) Deshaies, R. J., and Joazeiro, C. A. (2009) RING domain E3 ubiquitin ligases. *Annu. Rev. Biochem. 78*, 399−434.

(6) Huibregtse, J. M., Scheffner, M., Beaudenon, S., and Howley, P. M. (1995) A family of proteins structurally and functionally related to the E6-AP ubiquitin-protein ligase. *Proc. Natl. Acad. Sci. U.S.A. 92*, 2563−2567.

(7) Wenzel, D. M., Lissounov, A., Brzovic, P. S., and Klevit, R. E. (2011) UBCH7 reactivity profile reveals parkin and HHARI to be RING/HECT hybrids. *Nature 474*, 105−108.

(8) Ciechanover, A., and Ben-Saadon, R. (2004) N-terminal ubiquitination: More protein substrates join in. *Trends Cell Biol. 14*, 103−106.

(9) Ye, Y., and Rape, M. (2009) Building ubiquitin chains: E2 enzymes at work. *Nat. Rev. Mol. Cell Biol. 10*, 755−764.

(10) David, Y., Ziv, T., Admon, A., and Navon, A. (2010) The E2 ubiquitin-conjugating enzymes direct polyubiquitination to preferred lysines. *J. Biol. Chem. 285*, 8595−8604.

(11) Kim, H. C., and Huibregtse, J. M. (2009) Polyubiquitination by HECT E3s and the determinants of chain type specificity. *Mol. Cell. Biol. 29*, 3307−3318.

(12) Christensen, D. E., Brzovic, P. S., and Klevit, R. E. (2007) E2-BRCA1 RING interactions dictate synthesis of mono- or specific polyubiquitin chain linkages. *Nat. Struct. Mol. Biol. 14*, 941−948.

(13) Capili, A. D., and Lima, C. D. (2007) Taking it step by step: Mechanistic insights from structural studies of ubiquitin/ubiquitin-like protein modification pathways. *Curr. Opin. Struct. Biol. 17*, 726−735.

(14) Duda, D. M., Borg, L. A., Scott, D. C., Hunt, H. W., Hammel, M., and Schulman, B. A. (2008) Structural insights into NEDD8 activation of cullin-RING ligases: Conformational control of conjugation. *Cell 134*, 995−1006.

(15) Huang, L., Kinnucan, E., Wang, G., Beaudenon, S., Howley, P. M., Huibregtse, J. M., and Pavletich, N. P. (1999) Structure of an E6AP-UbcH7 complex: Insights into ubiquitination by the E2-E3 enzyme cascade. *Science 286*, 1321−1326.

(16) Verdecia, M. A., Joazeiro, C. A., Wells, N. J., Ferrer, J. L., Bowman, M. E., Hunter, T., and Noel, J. P. (2003) Conformational flexibility underlies ubiquitin ligation mediated by the WWP1 HECT domain E3 ligase. *Mol. Cell 11*, 249−259.

(17) Ozkan, E., Yu, H., and Deisenhofer, J. (2005) Mechanistic insight into the allosteric activation of a ubiquitin-conjugating enzyme by RING-type ubiquitin ligases. *Proc. Natl. Acad. Sci. U.S.A. 102*, 18890−18895.

(18) Wenzel, D. M., Stoll, K. E., and Klevit, R. E. (2011) E2s: Structurally economical and functionally replete. *Biochem. J. 433*, 31−42.

(19) Eddins, M. J., Carlile, C. M., Gomez, K. M., Pickart, C. M., and Wolberger, C. (2006) Mms2-Ubc13 covalently bound to ubiquitin reveals the structural basis of linkage-specific polyubiquitin chain formation. *Nat. Struct. Mol. Biol. 13*, 915−920.

(20) Kamadurai, H. B., Souphron, J., Scott, D. C., Duda, D. M., Miller, D. J., Stringer, D., Piper, R. C., and Schulman, B. A. (2009) Insights into ubiquitin transfer cascades from a structure of a UbcH5B approximately ubiquitin-HECT(NEDD4L) complex. *Mol. Cell 36*, 1095−1102.

(21) Sakata, E., Satoh, T., Yamamoto, S., Yamaguchi, Y., Yagi-Utsumi, M., Kurimoto, E., Tanaka, K., Wakatsuki, S., and Kato, K. (2010) Crystal structure of UbcH5b∼ubiquitin intermediate: Insight into the formation of the self-assembled E2∼Ub conjugates. *Structure 18*, 138−147.

(22) Hamilton, K. S., Ellison, M. J., Barber, K. R., Williams, R. S., Huzil, J. T., McKenna, S., Ptak, C., Glover, M., and Shaw, G. S. (2001) Structure of a conjugating enzyme-ubiquitin thiolester intermediate reveals a novel role for the ubiquitin tail. *Structure 9*, 897−904.

(23) Serniwka, S. A., and Shaw, G. S. (2009) The structure of the UbcH8-ubiquitin complex shows a unique ubiquitin interaction site. *Biochemistry 48*, 12169−12179.

(24) Pruneda, J. N., Stoll, K. E., Bolton, L. J., Brzovic, P. S., and Klevit, R. E. (2011) Ubiquitin in motion: Structural studies of the ubiquitin-conjugating enzyme∼ubiquitin conjugate. *Biochemistry 50*, 1624−1633.

(25) Brzovic, P. S., Lissounov, A., Christensen, D. E., Hoyt, D. W., and Klevit, R. E. (2006) A UbcH5/ubiquitin noncovalent complex is required for processive BRCA1-directed ubiquitination. *Mol. Cell 21*, 873−880.

(26) Capili, A. D., and Lima, C. D. (2007) Structure and analysis of a complex between SUMO and Ubc9 illustrates features of a conserved E2-Ubl interaction. *J. Mol. Biol. 369*, 608−618.

(27) Choi, Y. S., Jeon, Y. H., Ryu, K. S., and Cheong, C. (2009) 60th residues of ubiquitin and Nedd8 are located out of E2-binding surfaces, but are important for K48 ubiquitin-linkage. *FEBS Lett. 583*, 3323−3328.

(28) Das, R., Mariano, J., Tsai, Y. C., Kalathur, R. C., Kostova, Z., Li, J., Tarasov, S. G., McFeeters, R. L., Altieri, A. S., Ji, X., Byrd, R. A., and Weissman, A. M. (2009) Allosteric activation of E2-RING finger-mediated ubiquitylation by a structurally defined specific E2-binding region of gp78. *Mol. Cell 34*, 674−685.

(29) Knipscheer, P., van Dijk, W. J., Olsen, J. V., Mann, M., and Sixma, T. K. (2007) Noncovalent interaction between Ubc9 and SUMO promotes SUMO chain formation. *EMBO J. 26*, 2797−2807.

(30) Li, W., Tu, D., Li, L., Wollert, T., Ghirlando, R., Brunger, A. T., and Ye, Y. (2009) Mechanistic insights into active site-associated polyubiquitination by the ubiquitin-conjugating enzyme Ube2g2. *Proc. Natl. Acad. Sci. U.S.A. 106*, 3722−3727.

(31) Brzovic, P. S., Keeffe, J. R., Nishikawa, H., Miyamoto, K., Fox, D., III, Fukuda, M., Ohta, T., and Klevit, R. (2003) Binding and recognition in the assembly of an active BRCA1/BARD1 ubiquitin-ligase complex. *Proc. Natl. Acad. Sci. U.S.A. 100*, 5646−5651.

(32) Xu, Z., Kohli, E., Devlin, K. I., Bold, M., Nix, J. C., and Misra, S. (2008) Interactions between the quality control ubiquitin ligase CHIP and ubiquitin conjugating enzymes. *BMC Struct. Biol. 8*, 26.

(33) Pflugrath, J. W. (1999) The finer things in X-ray diffraction data collection. *Acta Crystallogr. D55*, 1718−1725.

(34) McCoy, A. J., Grosse-Kunstleve, R. W., Adams, P. D., Winn, M. D., Storoni, L. C., and Read, R. J. (2007) Phaser crystallographic software. *J. Appl. Crystallogr. 40*, 658−674.

(35) Adams, P. D., Afonine, P. V., Bunkoczi, G., Chen, V. B., Davis, I. W., Echols, N., Headd, J. J., Hung, L. W., Kapral, G. J., Grosse-Kunstleve, R. W., McCoy, A. J., Moriarty, N. W., Oeffner, R., Read, R. J., Richardson, D. C., Richardson, J. S., Terwilliger, T. C., and Zwart, P. H. (2010) PHENIX: A comprehensive Python-based system for macromolecular structure solution. *Acta Crystallogr. D66*, 213−221.

(36) Terwilliger, T. C. (2003) SOLVE and RESOLVE: Automated structure solution and density modification. *Methods Enzymol. 374*, 22−37.

(37) Emsley, P., Lohkamp, B., Scott, W. G., and Cowtan, K. (2010) Features and development of Coot. *Acta Crystallogr. D66*, 486−501.

(38) Painter, J., and Merritt, E. A. (2006) Optimal description of a protein structure in terms of multiple groups undergoing TLS motion. *Acta Crystallogr. D62*, 439−450.

(39) DeLano, W. (2002) *The PyMol Molecular Graphics System*, DeLano Scientific, San Carlos, CA.

(40) Chen, V. B., Arendall, W. B., III, Headd, J. J., Keedy, D. A., Immormino, R. M., Kapral, G. J., Murray, L. W., Richardson, J. S., and Richardson, D. C. (2010) MolProbity: All-atom structure validation for macromolecular crystallography. *Acta Crystallogr. D66*, 12−21.
(41) Davis, I. W., Leaver-Fay, A., Chen, V. B., Block, J. N., Kapral, G. J., Wang, X., Murray, L. W., Arendall, W. B., III, Snoeyink, J., Richardson, J. S., and Richardson, D. C. (2007) MolProbity: All-atom contacts and structure validation for proteins and nucleic acids. *Nucleic Acids Res. 35*, W375−W383.
(42) Cock, P. J., Antao, T., Chang, J. T., Chapman, B. A., Cox, C. J., Dalke, A., Friedberg, I., Hamelryck, T., Kauff, F., Wilczynski, B., and de Hoon, M. J. (2009) Biopython: Freely available Python tools for computational molecular biology and bioinformatics. *Bioinformatics 25*, 1422−1423.
(43) Hunter, J. D. (2007) Matplotlib: A 2D Graphics Environment. *Comput. Sci. Eng. 9*, 90−95.
(44) Winget, J. M., and Mayor, T. (2010) The diversity of ubiquitin recognition: Hot spots and varied specificity. *Mol. Cell 38*, 627−635.
(45) Wickliffe, K. E., Lorenz, S., Wemmer, D. E., Kuriyan, J., and Rape, M. (2011) The mechanism of linkage-specific ubiquitin chain elongation by a single-subunit E2. *Cell 144*, 769−781.
(46) Schmitz, C., Stanton-Cook, M. J., Su, X. C., Otting, G., and Huber, T. (2008) Numbat: An interactive software tool for fitting Deltachi-tensors to molecular coordinates using pseudocontact shifts. *J. Biomol. NMR 41*, 179−189.
(47) Valafar, H., and Prestegard, J. H. (2004) REDCAT: A residual dipolar coupling analysis tool. *J. Magn. Reson. 167*, 228−241.
(48) Winkler, H., Zhu, P., Liu, J., Ye, F., Roux, K. H., and Taylor, K. A. (2009) Tomographic subvolume alignment and subvolume classification applied to myosin V and SIV envelope spikes. *J. Struct. Biol. 165*, 64−77.
(49) Vriend, G. (1990) WHAT IF: A molecular modeling and drug design program. *J. Mol. Graphics 8*, 29 , 52−56.
(50) Bocik, W. E., Sircar, A., Gray, J. J., and Tolman, J. R. (2011) Mechanism of polyubiquitin chain recognition by the human ubiquitin conjugating enzyme Ube2g2. *J. Biol. Chem. 286*, 3981−3991.
(51) Miura, T., Klaus, W., Gsell, B., Miyamoto, C., and Senn, H. (1999) Characterization of the binding interface between ubiquitin and class I human ubiquitin-conjugating enzyme 2b by multidimensional heteronuclear NMR spectroscopy in solution. *J. Mol. Biol. 290*, 213−228.
(52) Bosanac, I., Phu, L., Pan, B., Zilberleyb, I., Maurer, B., Dixit, V. M., Hymowitz, S. G., and Kirkpatrick, D. S. (2011) Modulation of K11-linkage formation by variable loop residues within UbcH5A. *J. Mol. Biol. 408*, 420−431.
(53) Krissinel, E., and Henrick, K. (2007) Inference of macromolecular assemblies from crystalline state. *J. Mol. Biol. 372*, 774−797.
(54) Zhang, M., Windheim, M., Roe, S. M., Peggie, M., Cohen, P., Prodromou, C., and Pearl, L. H. (2005) Chaperoned ubiquitylation: Crystal structures of the CHIP U box E3 ubiquitin ligase and a CHIP-Ubc13-Uev1a complex. *Mol. Cell 20*, 525−538.
(55) Zheng, N., Schulman, B. A., Song, L., Miller, J. J., Jeffrey, P. D., Wang, P., Chu, C., Koepp, D. M., Elledge, S. J., Pagano, M., Conaway, R. C., Conaway, J. W., Harper, J. W., and Pavletich, N. P. (2002) Structure of the Cul1-Rbx1-Skp1-F boxSkp2 SCF ubiquitin ligase complex. *Nature 416*, 703−709.
(56) Saha, A., Lewis, S., Kleiger, G., Kuhlman, B., and Deshaies, R. J. (2011) Essential role for ubiquitin-ubiquitin-conjugating enzyme interaction in ubiquitin discharge from Cdc34 to substrate. *Mol. Cell 42*, 75−83.
(57) Hurley, J. H., Lee, S., and Prag, G. (2006) Ubiquitin-binding domains. *Biochem. J. 399*, 361−372.
(58) Garner, T. P., Strachan, J., Shedden, E. C., Long, J. E., Cavey, J. R., Shaw, B., Layfield, R., and Searle, M. S. (2011) Independent interactions of ubiquitin-binding domains in a ubiquitin-mediated ternary complex. *Biochemistry 50*, 9076−9087.
(59) Lee, S., Tsai, Y. C., Mattera, R., Smith, W. J., Kostelansky, M. S., Weissman, A. M., Bonifacino, J. S., and Hurley, J. H. (2006) Structural basis for ubiquitin recognition and autoubiquitination by Rabex-5. *Nat. Struct. Mol. Biol. 13*, 264−271.
(60) Wu, P. Y., Hanlon, M., Eddins, M., Tsui, C., Rogers, R. S., Jensen, J. P., Matunis, M. J., Weissman, A. M., Wolberger, C., and Pickart, C. M. (2003) A conserved catalytic residue in the ubiquitin-conjugating enzyme family. *EMBO J. 22*, 5241−5250.
(61) Reverter, D., and Lima, C. D. (2005) Insights into E3 ligase activity revealed by a SUMO-RanGAP1-Ubc9-Nup358 complex. *Nature 435*, 687−692.
(62) Geurink, P. P., El Oualid, F., Jonker, A., Hameed, D. S., and Ovaa, H. (2012) A General Chemical Ligation Approach Towards Isopeptide-Linked Ubiquitin and Ubiquitin-Like Assay Reagents. *ChemBioChem 13*, 293−297.
(63) Castaneda, C., Liu, J., Chaturvedi, A., Nowicka, U., Cropp, T. A., and Fushman, D. (2011) Nonenzymatic assembly of natural polyubiquitin chains of any linkage composition and isotopic labeling scheme. *J. Am. Chem. Soc. 133*, 17855−17868.
(64) El Oualid, F., Merkx, R., Ekkebus, R., Hameed, D. S., Smit, J. J., de Jong, A., Hilkmann, H., Sixma, T. K., and Ovaa, H. (2010) Chemical synthesis of ubiquitin, ubiquitin-based probes, and diubiquitin. *Angew. Chem., Int. Ed. 49*, 10149−10153.
(65) Weiss, M. (2001) Global indicators of X-ray data quality. *J. Appl. Crystallogr. 34*, 130−135.